

SENSITIVITY ANALYSIS IN A FATIGUE DELAMINATION PROBLEM OF AN ELASTIC TWO-LAYER COMPOSITE

Ł. Figiel¹⁾, B. Lauke²⁾, M. Kamiński³⁾

¹⁾ **Department of Engineering Science, University of Oxford, Parks Road**
OX1 3PJ, Oxford, United Kingdom

²⁾ **Leibniz Institute of Polymer Research Dresden**
Hohe Str. 6, 01069, Dresden, Germany

³⁾ **Chair of Mechanics of Materials, Technical University of Łódź**
Al. Politechniki 6, 93-590, Łódź, Poland

Several parameters can affect the fatigue delamination growth in laminates – these include e.g. constituent material properties and/or composite shape. Knowledge about effects of these parameters can lead to a better understanding of the fatigue delamination behaviour and can also pinpoint directions for optimum composite design. These effects can be elucidated by carrying out an appropriate sensitivity analysis. A FEM-based computational approach to sensitivity analysis is proposed in this work to study composite parameter effects in a fatigue delamination problem of an elastic two-layer composite. It is used to calculate and analyse sensitivity gradients of the fracture parameter and fatigue cycle number with respect to composite design parameters such as layer elastic constants. It is observed that sensitivities computed from this approach are generally numerically stable. Obtained sensitivities pinpoint quantitatively the most and least important composite parameters that govern a fatigue delamination process. Sensitivity results are verified by another computational approach and a very good agreement is found.

Key words: layered structures, fatigue delamination, sensitivity analysis, finite element analysis.

1. INTRODUCTION

Composite laminates, such as classical fibre-reinforced laminates or hybrid composites, are utilised in many fields of modern engineering, where they are subjected to either static or cyclic (fatigue) loads [1]. The most common mode of failure of these materials is interlaminar fracture (delamination). Delamination growth can lead to a loss of structural integrity and hence – to catastrophic composite failure [2]. Therefore, a large amount of research, both experimental and theoretical, has been already undertaken to better understand that phenomenon under applied static or cyclic loads.

It is known that several factors can affect delamination growth such as environmental conditions, constituent material properties or a component geometry [3–5]. However, to the best knowledge of the authors there has not yet been carried out any detailed research concerning effects of these parameters on the fatigue delamination behaviour of composite laminates. The authors believe that it is necessary for a better understanding of a delamination phenomenon and for further, improved design and optimisation of layered materials. Therefore, an attempt to elucidate the effects of composite parameters is undertaken in this work by exploiting a concept of sensitivity analysis [6].

The sensitivity analysis is an introductory step to structural system optimisation [7] and reliability estimation [8]. Evaluation of sensitivities is a central point of the sensitivity analysis. These sensitivities map the changes of system design parameters (e.g. elastic constants or geometry) onto changes in the system objective parameters such as a composite effective property [9, 10] or composite fatigue life [11]. This in turn provides a relationship between design and objective parameter changes and enables to estimate the significance (or insignificance) of design parameters. This information can further be used in design optimisation of e.g. composite fatigue performance [12] or probabilistic fatigue analysis [13]. The sensitivities can be obtained using various approaches, e.g. by analytical derivation of partial derivatives, by finite difference approximation of partial derivatives, by automatic differentiation of numerical procedure, by computational implementation of explicit differentiation in the finite element method (FEM) codes or some probabilistic approaches [6, 8, 14–19]; utilisation and efficiency of each of these approaches depends on the boundary value problem at hand. From the engineering point of view, the sensitivity analysis is particularly very useful, when it is formulated in the framework of one of the numerical methods such as the finite element method (FEM) or the boundary element method (BEM). The advanced state of the FEM and related software provides a reliable tool for composite analysis, but it gives a composite engineer only little help in identifying the ways to modify composite design to improve the desired qualities. Using the design sensitivity information generated by strategies exploiting the FEM formulation and software, the composite engineer would be able to carry out a systematic trade-off analysis and improve the composite design.

The main goal of this paper is to present a computational approach for calculation and analysis of sensitivities for a fatigue delamination problem of an elastic two-component laminate. This approach combines a fatigue delamination model with the concept of finite differences and it is implemented using the FEM-based program ANSYS. The developed approach is used to compute sensitivities of the total energy release rate and fatigue life, to reveal the most crucial design parameters of a two-component composite laminate. This paper starts with a description of the fatigue delamination model and sensitivity calcu-

lation with finite differences. Further, computer implementation of the approach is presented. A computational illustration utilising a two-component laminate subjected to cyclic shear loads is presented and discussed.

2. FATIGUE DELAMINATION MODEL AND SENSITIVITIES

A composite system composed of two layers, Ω_1 and Ω_2 is considered here and shown in Fig. 1. The two layers are assumed as isotropic linear-elastic materials defined by the elasticity tensor C_n in terms of two elastic engineering constants, i.e. Young's modulus E_n and Poisson's ratio ν_n , and n denotes the n -th ($n = 1, 2$ in this work). It is assumed that there exists a delamination over some portion of a curved interface between those two layers, denoted by $\Gamma_{c(n)}$. The other part of the curved interface is assumed as perfectly bonded and denoted by Γ_I . The interface itself is assumed to have a vanishing thickness, i.e. $t_I \rightarrow 0$ and its curvature is denoted by a radius R_I .

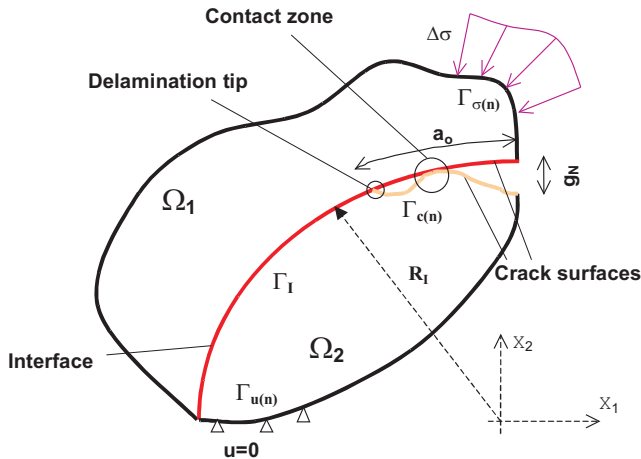


FIG. 1. Two-component model of a delaminated composite laminate.

The composite system is subjected to cyclic loads of constant amplitude $\Delta\sigma = \sigma_{\max} - \sigma_{\min} = \text{const.}$ and load ratio $R = \sigma_{\min}/\sigma_{\max} = 0$ applied to the composite boundary $\Gamma_{\sigma(n)}$ (cf. Fig. 1); σ_{\max} and σ_{\min} denote the maximum and minimum values of applied loads. The composite is supported on the portion of its boundary denoted by $\Gamma_{u(n)}$ (cf. Fig. 1).

It is assumed that under these boundary conditions the fatigue delamination growth per cycle N can be described by the modified Paris law as follows:

$$(2.1) \quad \frac{da}{dN} = C(G_T)^m,$$

where G_T is the total energy release rate (the crack driving force parameter) such that $G_T = \Delta G_T = G_{T,\max}$ – it is assumed that the minimum total energy release rate at a cycle does not influence the fatigue delamination growth under $R = 0$ ($G_{T,\min} = 0$). Then, C and m are the empirical constants. The model describes a stable fatigue crack growth along the selected crack path.

Then, two situations that can occur at the delamination tip during propagation under applied fatigue load are considered in this work, i.e. 1) opened and 2) closed delamination tips as shown in Fig. 2.

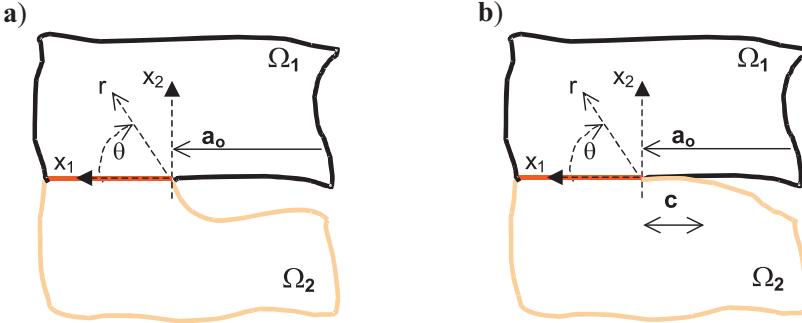


FIG. 2. Near-tip behaviour during fatigue delamination a) opened crack tip
b) closed crack tip.

In the case when the tip is opened during propagation, i.e. when the gap g_N at the tip is larger than zero (cf. Fig. 1), the stress distribution around the tip is assumed to be governed by the so-called oscillatory solution of the linear fracture mechanics for interface cracks [21]. In addition, since the crack propagation along the interface (without kinking out or branching) is analysed here, therefore it is sufficient to account for stresses ahead of the delamination tip i.e. for $\theta = 0$ as follows:

$$(2.2) \quad \sigma_{22(t)} + i\sigma_{12(t)} = \frac{1}{\sqrt{2\pi r}} (K_1 + iK_2) r_o^{i\varepsilon} \left(\frac{r}{r_o}\right)^{i\varepsilon},$$

where $\sigma_{22(t)}$ and $\sigma_{12(t)}$ denote normal and shear stresses near the delamination tip – since $R = 0$ then $\sigma_{ij(t)} = \Delta\sigma_{ij(t)} = \sigma_{ij(t,\max)}$, where $\sigma_{ij(t,\max)}$ denotes the tip stresses at the maximum applied load during a single cycle. Then, K_1 and K_2 are real and imaginary components of the complex stress intensity factor K , which similarly to crack tip stresses correspond to maximum load in a single cycle. Further, r_o is a characteristic length as an attempt to produce dimensionally meaningful results for K_1 and K_2 . Finally, ε is an oscillation index (or mismatch parameter) given as follows [21]:

$$(2.3) \quad \varepsilon = \frac{1}{2\pi} \ln \left(\frac{1 - \beta}{1 + \beta} \right),$$

where β is the second Dundurs mismatch parameter given by

$$(2.4) \quad \beta = \frac{\mu_1 (\kappa_2 - 1) - \mu_2 (\kappa_1 - 1)}{\mu_1 (\kappa_2 + 1) + \mu_2 (\kappa_1 + 1)},$$

where μ_n is the shear modulus and κ_n denotes the Kolosov constant such that $\kappa_n = 3 - 4\nu_n$ for plane strain conditions and $\kappa_n = (3 - \nu_n)/(1 + \nu_n)$ under plane stress conditions; n denotes the n -th layer.

Then, for the cyclic variation of applied stress and $R = 0$, propagation of a delamination with an opened tip is controlled by the total energy release rate, expressed as follows:

$$(2.5) \quad G_T = \frac{(1 - \beta^2)}{E^{\text{eff}}} \left[(K_1)^2 + (K_2)^2 \right],$$

where the effective Young's modulus E^{eff} is given by

$$(2.6) \quad E^{\text{eff}} = \frac{2\bar{E}_1\bar{E}_2}{\bar{E}_1 + \bar{E}_2},$$

where $\bar{E}_n = E_n / (1 - \nu_n)^2$ under plane strain conditions and $\bar{E}_n = E_n$ under plane stress conditions. In order to calculate the total energy release rate one needs to know K_1 and K_2 . They can be obtained from stresses (Eq. (2.2)) and the well-known Euler relations

$$(2.7) \quad e^{i\varphi} = \cos \varphi + i \sin \varphi \quad \text{and} \quad e^{-i\varphi} = \cos \varphi - i \sin \varphi,$$

as follows:

$$(2.8) \quad K_1 = \sqrt{2\pi r} \left\{ \sigma_{22(t)} \cos \left(\varepsilon \ln \left[\frac{r}{r_o} \right] \right) + \sigma_{12(t)} \sin \left(\varepsilon \ln \left[\frac{r}{r_o} \right] \right) \right\},$$

$$(2.9) \quad K_2 = \sqrt{2\pi r} \left\{ \sigma_{12(t)} \cos \left(\varepsilon \ln \left[\frac{r}{r_o} \right] \right) - \sigma_{22(t)} \sin \left(\varepsilon \ln \left[\frac{r}{r_o} \right] \right) \right\}.$$

In the case when the delamination propagates with a closed tip (cf. Fig. 2b), i.e. when the gap g_N at the crack tip equals zero (cf. Fig. 1) and delamination surfaces slide over each other, shear stresses along the interface ahead of the crack tip are assumed to have the following form:

$$(2.10) \quad \sigma_{12(t)} = \frac{K_2}{(2\pi r)^\lambda},$$

where λ describes a stress singularity that depends on the friction coefficient f in the following way:

$$(2.11) \quad \cot(\lambda\pi) = f\beta,$$

where β is described by Eq. (2.4).

Then, the delamination propagation with a closed tip under applied cyclic loads of $R = 0$ is governed by the following total energy release rate [22]:

$$(2.12) \quad G_T = \frac{(K_2)^2 \sin \lambda\pi}{2\gamma(1-\lambda)(2\pi)^{2\lambda}} \Delta a^{1-2\lambda} \left[\frac{\Gamma(2-\lambda)\Gamma(1-\lambda)}{\Gamma(3-2\lambda)} - \frac{\cos \lambda\pi}{2(1-\lambda)} \right],$$

where γ is a parameter described in terms of μ_n , κ_n and β and given by

$$(2.13) \quad \gamma = \frac{4\mu_1\mu_2}{\mu_2\kappa_1(1+\beta) + \kappa_2\mu_1(1-\beta) + 2},$$

and $\Gamma(\cdot)$ is the Euler gamma function. The delamination driving force G_T described in Eq. (2.12) is dependent on the crack extension, Δa , which must be finite because G_T diminishes as $\Delta a \rightarrow 0$ and $\lambda < 0.5$, while it becomes unbounded as $\Delta a \rightarrow 0$ and $\lambda > 0.5$ as reported in [22].

Then, the fatigue life of a delaminated composite can be predicted by integrating Eq. (2.1) from an initial delamination length, a_o , to the one that corresponds to a composite failure, a_f , as follows:

$$(2.14) \quad N_f = \int_{a_o}^{a_f} \frac{da}{C(G_T)^m}.$$

In order to determine numerically the fatigue cycles number at failure, the delamination length range from a_o to a_f is divided into equal crack increments, $\Delta a = a_{i+1} - a_i$. Hence, the fatigue life is obtained as the sum of all fatigue cycle number increments as follows:

$$(2.15) \quad N_f = \sum_{i=1}^n N_i \quad \text{and} \quad N_i = \int_{a_i}^{a_{i+1}} \frac{da}{C(G_T(a_i))^m}.$$

As it can be seen directly from Eqs. (2.14) and (2.15), the fatigue life or increment of fatigue cycles depends on the initial delamination length a_o , constants C and m , the crack driving force G_T and material properties such as the n -th layer Young's modulus E_n . The sensitivity analysis allows to estimate the influence of each model parameter on the fracture parameter, fatigue cycle increment during delamination propagation, and finally on the composite fatigue life. In this

work, that influence is estimated in terms of sensitivity gradients (sensitivities). The sensitivity gradients of the composite fatigue life are approximated by the forward finite difference as follows:

$$(2.16) \quad S = \frac{N_f(b_k + \Delta b_k) - N_f(b_k)}{\Delta b_k}$$

or by an alternative expression using the central finite difference

$$(2.17) \quad S = \frac{N_f(b_k + \Delta b_k) - N_f(b_k - \Delta b_k)}{2\Delta b_k},$$

where b_k denotes a nominal value of a design parameter such as E_n or h_n and Δb_k is an infinitesimally small variation of a design parameter about its nominal value b_k .

The main issue related to sensitivity calculations through finite and central difference approaches is the numerical stability (or instability) of sensitivities. Therefore, a proper choice of the design parameter increment, Δb_k , is required. The main advantage of the central finite difference approximation over the forward one is that it allows a larger value of Δb_k to be selected. This also permits avoiding problems associated with small parameter increments, such as numerical round-offs. However in practice, it is usually possible to find an appropriate parameter increment associated with the forward finite difference that provides numerically stable sensitivities.

Eqs. (2.16)–(2.17) express a sensitivity measure, which is inconvenient in cases where sensitivities of N_f with respect to different design parameters must be characterised and compared. Since it is the case in this work, thus, the relative sensitivity or classical sensitivity due to BODE [23] is utilised here and given by

$$(2.18) \quad S_{\text{rel}} = \frac{\partial(\ln N_f)}{\partial(\ln b_k)} = \frac{\partial N_f / N_f}{\partial b_k / b_k} = \frac{\partial N_f}{\partial b_k} \frac{b_k}{N_f},$$

which provides a dimensionless sensitivity measure appropriate for comparative purposes. It is mentioned that an analogous expression for the fracture parameter G_T can be obtained by replacing N_f .

It must be mentioned that in this work, the sensitivities are calculated with respect to a single parameter change, Δb_k , i.e. only a single design parameter is subjected to a perturbation when the sensitivity is calculated. Calculation of sensitivities, when more than one design parameter is perturbed, would be more general, but it should account for some correlations between particular design parameters. In that case it might be more appropriate to use a probabilistic approach for calculation of sensitivities [24] rather than the current concept.

3. COMPUTER IMPLEMENTATION USING ANSYS

Efficient numerical evaluation of relative sensitivities, given by Eq. (2.18), demands a development of a numerical approach and its computer implementation. In this work, the FEM is chosen as a tool to solve a boundary value problem for displacements, and then strains and stresses. Hence, the fatigue delamination model and relevant equations for sensitivity measure are combined together and implemented into the FEM-based package ANSYS. In particular, the advantage is taken of the ANSYS Parametric Design Language (APDL), which permits obtaining sensitivities from equations coded up in the postprocessor. Hence, this implementation does not demand any access to the source code of ANSYS.

A numerical strategy proposed to compute sensitivities in this work, is sketched schematically in Fig. 3 and described below in a detail.

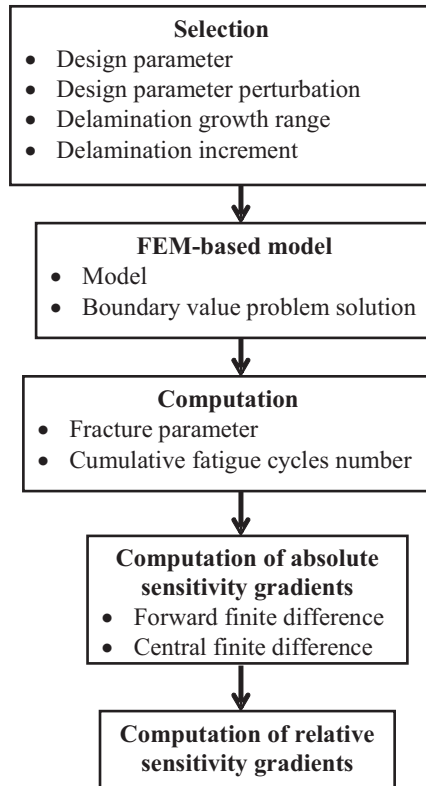


FIG. 3. Flowchart for computation of sensitivities.

The first step is to select a design parameter (e.g. layer Young's modulus), its perturbation as well as to define delamination propagation range (using a_o and a_f) and delamination increment (Δa_i). In the next step, a FEM model of

the problem must be built using a pre-processor of ANSYS. Each FEM model parameter such as material or geometrical parameter is defined parametrically to allow for a full flexibility for sensitivity computations. Then, a boundary value problem needs to be solved using the FEM for a selected design parameter value and its increment, at required delamination lengths. Hence, considering a two-layer composite with a delamination (Fig. 1) subjected to arbitrarily prescribed loads, one needs to solve the following general differential boundary value problem:

$$(3.1) \quad \text{Div}(\boldsymbol{\sigma}_n) = 0 \quad \mathbf{x} \in \Omega_n,$$

$$(3.2) \quad \boldsymbol{\varepsilon}_n = \frac{1}{2} [\nabla(\mathbf{u}_n) + \nabla(\mathbf{u}_n)^T] \quad \mathbf{x} \in \Omega_n,$$

$$(3.3) \quad \boldsymbol{\sigma}_n = \mathbf{C}_n \boldsymbol{\varepsilon}_n \quad \mathbf{x} \in \Omega_n,$$

$$(3.4) \quad \boldsymbol{\sigma}_n \mathbf{n}_n = \mathbf{t}_n \quad \mathbf{x} \in \Gamma_{\sigma(n)},$$

$$(3.5) \quad \mathbf{u}_n = 0 \quad \mathbf{x} \in \Gamma_{u(n)},$$

$$(3.6) \quad \tau = f|p| \quad \text{for} \quad g_N \leq 0 \quad \mathbf{x} \in \Gamma_{c(n)},$$

$$(3.7) \quad \tau = p = 0 \quad \text{for} \quad g_N > 0 \quad \mathbf{x} \in \Gamma_{c(n)},$$

where $\boldsymbol{\sigma}_n = \boldsymbol{\sigma}_n(b_k)$ is the stress tensor at a point in the interior of the n -th composite constituent Ω_n ; $\boldsymbol{\varepsilon}_n = \boldsymbol{\varepsilon}_n(b_k)$ is the strain tensor written in terms of the displacement field in $\mathbf{u}_n = \mathbf{u}_n(b_k)$; \mathbf{n}_n is the unit vector that is normal to the surface of the composite constituent; \mathbf{t}_n denotes the applied surface tractions on $\Gamma_{\sigma(n)}$; f is the friction coefficient that approximates roughness of delaminated composite parts (contact surfaces); p and τ denote the contact pressure and frictional stresses along the crack surfaces remaining in contact.

The boundary value problem (3.1)–(3.7) is complemented by conditions of stress equilibrium (normal and shear components only) and continuity of displacement across the uncracked portion of the interface, denoted by Γ_I . It should be mentioned that the boundary value problem presented above is general, and its specific form, i.e. under prescribed shear loads, is solved using ANSYS in this work.

The problem is primarily solved for displacements, and then strains and stresses are computed for each value of the design parameter b_k . Then, the total energy release rate, G_T , can be obtained using crack-tip stresses from Eqs. (2.8)–(2.9), what in turn enables calculation of the fatigue cycles number, N_f . It is mentioned that stress intensity factors K_1 and K_2 required to calculate

G_T are obtained by a linear extrapolation of stress intensity factors determined at finite element nodes at $\theta = 0$ over a selected distance r (cf. Fig. 2). The extrapolation technique is based on the least squares method to give

$$(3.8) \quad K_{1,2} = \frac{\sum_{i=1}^{n_k} K_{i(1,2)} - d \sum_{i=1}^{n_k} y_i}{n_k},$$

where

$$(3.9) \quad d = \frac{n_k \left(\sum_{i=1}^{n_k} K_{i(1,2)} y_i \right) - \left(\sum_{i=1}^{n_k} K_{i(1,2)} \right) \left(\sum_{i=1}^{n_k} y_i \right)}{n_k \left(\sum_{i=1}^{n_k} y_i^2 \right) - \left(\sum_{i=1}^{n_k} y_i \right)^2},$$

where y_i is the distance between the i -th node n_i and the delamination tip; n_k is the number of nodes used in the extrapolation of nodal stress intensity factors $K_{i(1,2)}$.

The boundary value problem described by Eqs. (3.1)–(3.7) is solved for a selected design parameter at subsequent crack lengths until the final delamination length a_f is reached. When that is the case, the entire procedure (i.e. solution of the boundary value problem and fracture parameter calculation as well as fatigue cycle increment) is repeated for a new design parameter increment. This is done to study the numerical stability of sensitivities calculated from the finite difference concept. Results of calculations, in terms of the fracture parameter and fatigue cycle number are written to output files at each delamination length and design parameter increment. After the computational procedure is completed for the last design parameter increment, then sensitivity calculations begin. The absolute sensitivities are calculated first, using forward and/or central finite difference methods. Then, relative sensitivities are obtained by appropriate scaling of absolute sensitivities according to Eq. (2.18). The entire computational process is repeated for all design parameters of interest. That process is coded up into ANSYS such that it does not need any user interference, when sensitivities are calculated for a single design parameter – i.e. the computational process is run automatically at each delamination length and design parameter perturbation until $a = a_f$. However for the time being, a change in the design parameter (e.g. Young's modulus) to the layer thickness must be done manually by the user.

The solution of the boundary value problem is the most expensive step of the approach, in terms of computational time. It will obviously be less expensive for linear elastic problem, while the computational costs will increase with introduction of geometrical and physical nonlinearities.

4. COMPUTATIONAL EXAMPLE

4.1. FEM model

Accuracy and applicability of the approach presented in the Sec. 3 is evaluated on an example related to a two-component boron/epoxy-aluminium (B/Ep-Al) curved composite (cf. Fig. 4). This composite laminate represents a simplified repeated element of a hybrid-like composite laminate, which is utilised in aerospace applications – frequently in large curved parts of the aircraft fuselage. Both layers have the same nominal thickness $h_1 = h_2 = 2.5 \times 10^{-3}$ m, then composite width is $w = 5 \times 10^{-3}$ m, while the interface curvature is described by the nominal radius value $R_I = 5.25 \times 10^{-2}$ m. B/Ep component is considered as a linear elastic and isotropic material with the Young modulus $E_1 = 207$ GPa and Poisson's ratio $\nu_1 = 0.21$. This is only a rough approximation to the real situation where B/Ep component behaves as an anisotropic and viscoelastic material, depending on the volume fraction of the boron reinforcement. The Al component is also considered as linear elastic and isotropic with the corresponding material properties $E_2 = 70.8$ GPa and $\nu_1 = 0.33$. Here the real situation is simplified by assuming that the yield stress of aluminum is very high. The interface is modelled as a zero thickness layer with no assigned material properties.

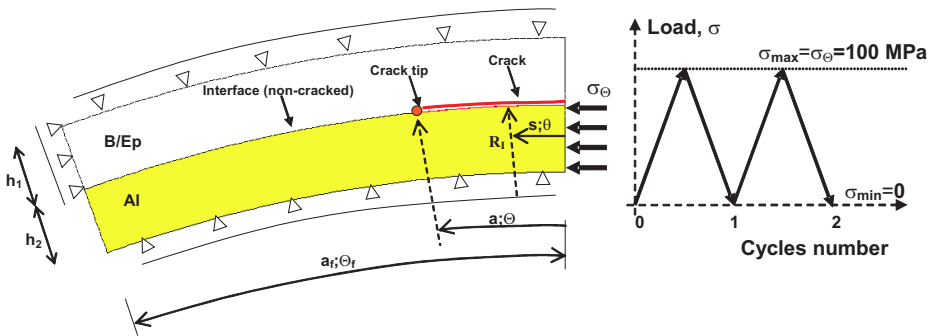


FIG. 4. Two-layer boron/epoxy-aluminium curved composite under cyclic shear.

The composite structure contains an initial delamination of length $a = a_o = 5.498 \times 10^{-3}$ m ($\Theta = \Theta_o = 6$ deg) located at the interface between layers. Then, the total interface length, including cracked and perfectly bonded parts of the interface, is equal to $a = a_f = 1.835 \times 10^{-2}$ m ($\Theta = \Theta_f = 20$ deg). The nominal value of the interface friction coefficient is selected arbitrarily and equal to $f = 0.05$. Then, the nominal value of the fatigue law exponent is equal to $m = 10$. The nominal value of the fatigue law constant is equal to $C = 1 \times 10^{-29}$ and it was evaluated based on the knowledge of the total energy

release rate threshold, $G_{T,th} = 100 \text{ J/m}^2$ as well as the delamination growth threshold, $(da/dN)_{th} = 1 \times 10^{-9} \text{ m/cycle}$ according to the concept reported in [25].

The composite laminate is subjected to cyclic shear loads with a triangular profile shown in Fig. 4. Shear type of loading is designed by constraining composite edges in the radial direction and additionally imposing supports on the upper component in the angular direction. The cyclic load of $\sigma_\theta = 100 \text{ MPa}$ is applied to lower composite constituent (with thickness h_2) in the angular direction. It is noted that the aforementioned boundary conditions simulate those of a proposed compression shear fracture test for curved and flat layered specimens [26].

Both layers are discretised by eight-node solid elements PLANE82, while the crack surfaces – by contact elements pairs CONTA172-TARGE169 as shown in Fig. 5. The mesh is designed here in such a way that the contact elements number changes only along with the crack length from 42 ($a/a_o = 1$) to 94 ($a/a_o = 3.167$), while the solid elements number is fixed and equal to 2224. Special attention is focused on the discretisation of the near-tip domain to simulate properly the stress singularity. A single row of quarter-point elements with radius $r_1 = 1 \times 10^{-6} \text{ m}$ discretises the crack tip vicinity and the mesh becomes coarser far away from the crack tip as shown in Fig. 5. Investigation of the influence of different r_1 values on the total energy release rate is shown in the following subsection.

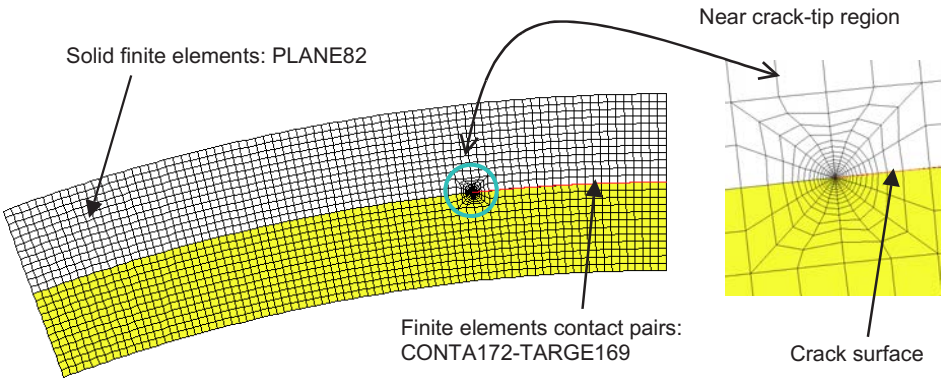


FIG. 5. FEM discretisation of composite domain and crack surfaces.

The augmented Lagrange method implemented in ANSYS was utilised to compute contact constraints. Computation of frictional stresses and resulting slip was possible with the so-called radial return algorithm available in ANSYS. Solution was obtained *via* the full Newton–Raphson incremental-iterative technique, and the line search option was used to enhance the solution convergence.

4.2. Total energy release rate

Accurate calculation of the total energy release rate is a key step in determination of fatigue cycle number and then proper evaluation of relative sensitivities of fracture parameter and fatigue life. Therefore, results obtained from the current model are verified by those obtained using the virtual crack closure method (VCCM) as reported in [27]. Mixed mode formulation of the VCCM for singular elements is used. Results are compared for three different values of $r_1 = 0.5 \times 10^{-6}$, 1×10^{-6} and 5×10^{-6} . It must be mentioned that a careful investigation of the delamination growth revealed that the crack tip was opened for all crack lengths under the considered boundary conditions. However, the delamination was opened only in the vicinity of the crack tip, while delaminated surfaces were in frictional contact with each other, away from the crack tip.

Table 1. Comparison of the fracture parameter G_T for $a/a_o = 1$.

r_1 [m]	G_T [J/m ²] (from Eq. (2.5))	G_T [J/m ²] (from the VCCT)
5×10^{-6}	123.826	118.603
1×10^{-6}	121.648	120.579
0.5×10^{-6}	120.661	127.466

Therefore, the fracture parameter was computed from Eq. (2.5) and its results are verified against those obtained from the VCCT, and shown in Table 1 for the normalised crack length $a/a_o = 1$. In addition, the fracture mode 2 of the fracture parameter, G_2 , prevails for all crack lengths, so $G_T \approx G_2$. Fracture parameter values obtained from Eq. (2.5) are only slightly sensitive to the value of r_1 as shown in Table 1, contrary to those obtained from the VCCT, which increase as r_1 decreases. However, a good agreement between these two approaches is obtained for $r_1 = 1 \times 10^{-6}$. Therefore, the total energy release rate determined from Eq. (2.5) and that value of r_1 is used in all sensitivity calculations.

4.3. Interpretation of sensitivity analysis results

Interpretation of sensitivity results is presented with some selected examples, where the relative sensitivity S_{rel} of the total energy release rate and the fatigue cycles number is obtained with respect to composite parameters. The sensitivities are calculated for three different parameter increments, 0.1%, 1% and 10%. A simple engineering interpretation of relative sensitivity gradients of the fracture parameter and fatigue cycle number, is that if a particular gradient is less than 0, an increase of composite parameter (e.g. layer Young's modulus) accompanies the reduction of the objective parameter (fracture parameter and/or fatigue cycle number). Otherwise (the relative sensitivity greater than 0), an increase of the design parameter results in an appropriate increase of the objective

parameter. Ultimately, if the sensitivity is comparable to 0, then the given design parameter does not influence the objective parameter.

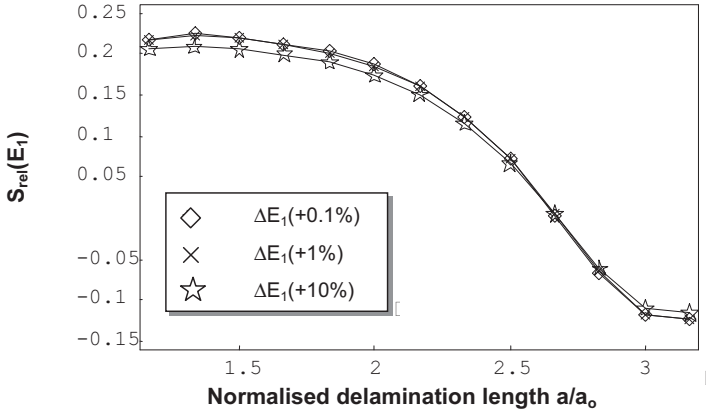


FIG. 6. Relative sensitivities of the fracture parameter with respect to the Young's modulus E_1 .

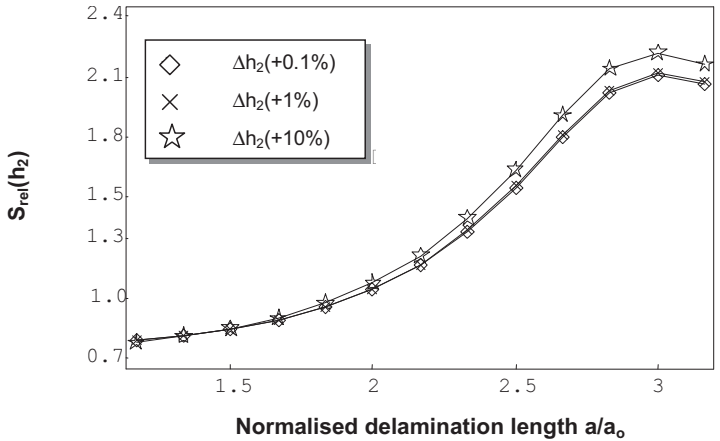


FIG. 7. Relative sensitivities of the fracture parameter with respect to the layer thickness h_2 .

For example, results of relative sensitivities of the total energy release rate with respect to the Young's modulus of the upper layer $S_{\text{rel}}(E_1)$, thickness of the lower layer $S_{\text{rel}}(h_2)$ and the interface radius $S_{\text{rel}}(R_I)$, are shown in Figs. 6–8, as functions of a normalised delamination length, a/a_0 . This enables to demonstrate evolution of relative sensitivities as the crack propagates. An interesting behaviour is shown in Fig. 6, where the relative sensitivity is positive at short delamination lengths and then changes its sign for large crack lengths. Thus, an increase of the upper layer Young modulus leads to an increase of the fracture

parameter at short delamination lengths, whereas an opposite situation (reduction of the fracture parameter for increasing Young's modulus) is observed at large crack lengths. Hence, there exists a point where the sensitivity equals zero so the fracture parameter value is not affected by the change of the investigated design parameter (the upper layer Young's modulus in this case). Then, the relative sensitivities of the total energy release rate with respect to the thickness of the lower layer, h_2 , are shown in Fig. 7. It is possible to observe from that figure that the fracture parameter increases with increasing layer thickness. Additionally, the relative sensitivities increase as the delamination propagates. A similar situation is observed in Fig. 8, where the relative sensitivities are positive during nearly entire range of crack growth (excluding some numerical instabilities near the shortest delamination length). However, a quantitative difference between results in Figs. 7 and 8 is observed. The relative sensitivities obtained with respect to the lower layer thickness (Fig. 7) are larger, at the order of two, than those calculated with respect to the interface radius (Fig. 8).

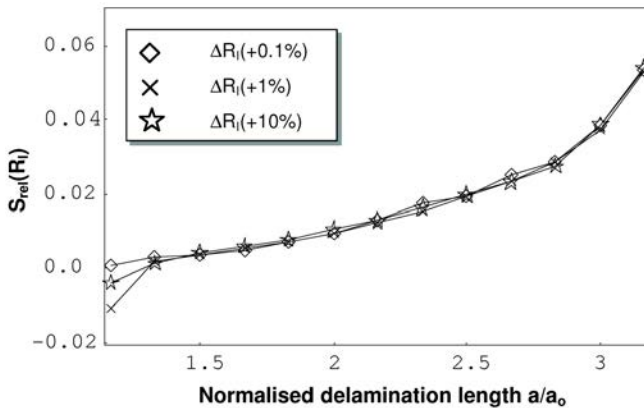


FIG. 8. Relative sensitivities of the fracture parameter with respect to the interface radius R_I .

Relative sensitivity results shown in Figs. 6–8 demonstrate usefulness of the sensitivity analysis in general. In particular, they enable to pinpoint exactly the importance of a particular composite parameter. In order to show that aspect in a more detail, the relative sensitivities of the fatigue cycles number were calculated with respect to several parameters and compared. Outcome of these computations is shown in Table 2 as a function of the normalised delamination length. Thus, the importance of each design parameter on the fatigue cycle number can be compared at consecutive delamination lengths. Here, it is only focused on the sensitivity values obtained at the largest crack length (last line of Table 2 marked in bold). These sensitivities enable to judge the importance of each parameter on the fatigue life of the analysed composite. It is shown in

Table 2 that two parameters associated with the lower component of the composite, i.e. Young's modulus E_2 and the thickness h_2 , are the most significant parameters for the fatigue life. In particular, positive value of the relative fatigue life sensitivity gradient, $S_{\text{rel}}(E_2)$, corresponds to the fact that an increase in the lower layer Young's modulus extends considerably the composite fatigue life. This is directly connected with the fact that by increasing the lower layer Young's modulus, E_2 , the normalised crack tip opening and tangential displacements decrease, as shown in Figs. 9 and 10 for two normalised crack lengths as a function of the arc length s ($s = 0$ for $a = 0$). This in turn, results in a reduction of stress component values around the crack tip (interestingly without a change of stress distribution) as shown in Fig. 12 for a single normalised delamination length, and compared with the reference (unperturbed) stress values in Fig. 11. Reduction of crack tip displacements and near tip stresses leads to a reduction of the crack driving force (total energy release rate), as demonstrated later, in Figs. 13 and 14, by negative values of relative sensitivities of the fracture parameter with respect to the lower layer Young's modulus, E_2 . Hence, altogether it leads to the conclusion that delamination demands more loading cycles to propagate from a_o to a_f with increasing E_2 . Thus, an increase in the component stiffness ratio E_2/E_1 might retard the fatigue failure of the analysed composite.

Table 2. Relative sensitivity gradients of the fatigue cycles number (parameter perturbation +1%).

a/a_o	$S_{\text{rel}}(E_1)$	$S_{\text{rel}}(E_2)$	$S_{\text{rel}}(\nu_1)$	$S_{\text{rel}}(\nu_2)$	$S_{\text{rel}}(h_1)$	$S_{\text{rel}}(h_2)$	$S_{\text{rel}}(\mu)$	$S_{\text{rel}}(R_I)$
1.167	-2.292	12.957	-1.662	3.016	-3.220	-8.732	0.814	-1.467
1.333	-2.210	13.060	-0.878	3.171	-3.202	-8.119	0.808	-0.638
1.500	-2.204	13.024	-0.620	3.216	-3.228	-8.004	0.918	-0.412
1.667	-2.192	12.993	-0.493	3.266	-3.258	-8.034	1.011	-0.305
1.833	-2.171	12.959	-0.415	3.312	-3.286	-8.144	1.096	-0.247
2.000	-2.139	12.914	-0.366	3.349	-3.313	-8.317	1.173	-0.215
2.167	-2.097	12.860	-0.333	3.372	-3.334	-8.535	1.238	-0.198
2.333	-2.049	12.801	-0.312	3.381	-3.347	-8.767	1.287	-0.191
2.500	-2.006	12.749	-0.300	3.378	-3.352	-8.957	1.316	-0.189
2.667	-1.982	12.721	-0.295	3.372	-3.351	-9.058	1.327	-0.189
2.833	-1.975	12.713	-0.294	3.370	-3.349	-9.082	1.329	-0.189
3.000	-1.974	12.713	-0.294	3.370	-3.349	-9.084	1.329	-0.189
3.167	-1.974	12.713	-0.294	3.370	-3.349	-9.084	1.329	-0.189
3.333	-1.974	12.713	-0.294	3.370	-3.349	-9.084	1.329	-0.189

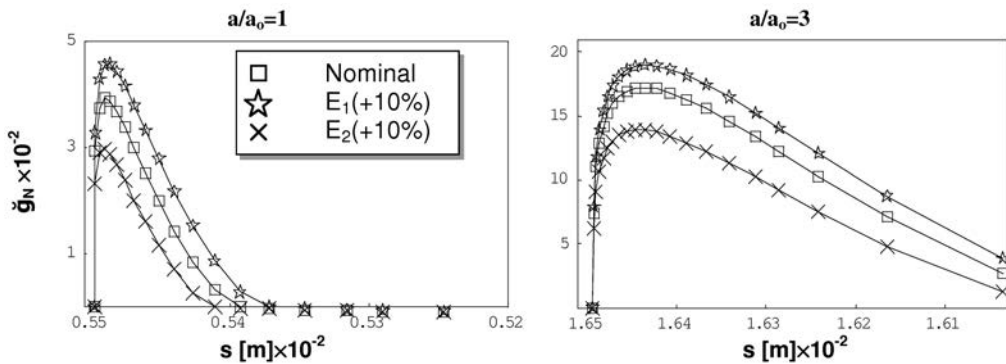


FIG. 9. Effects of Young's moduli variations on delamination tip opening displacements.

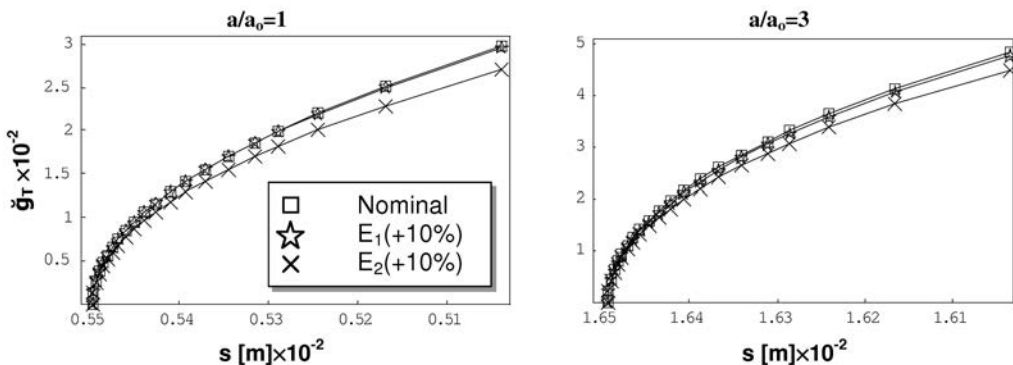


FIG. 10. Effects of Young's moduli variations on delamination tip tangential displacements.

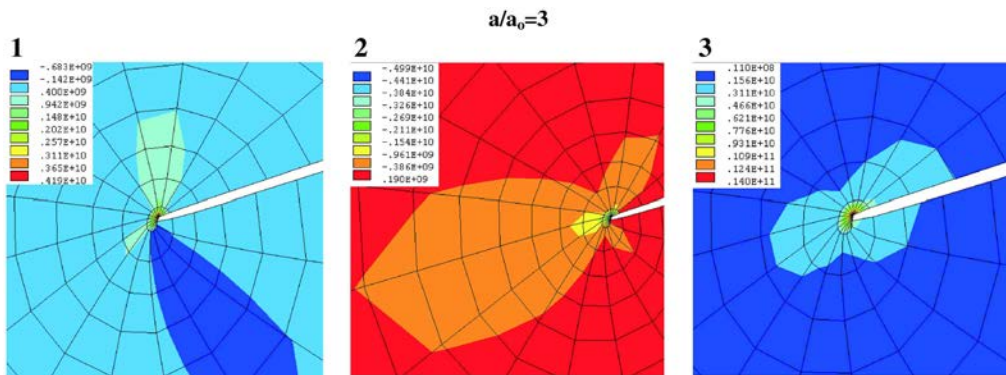


FIG. 11. Near-tip stress distribution for nominal design parameter values [Pa] (1) normal (2) shear (3) von Mises.

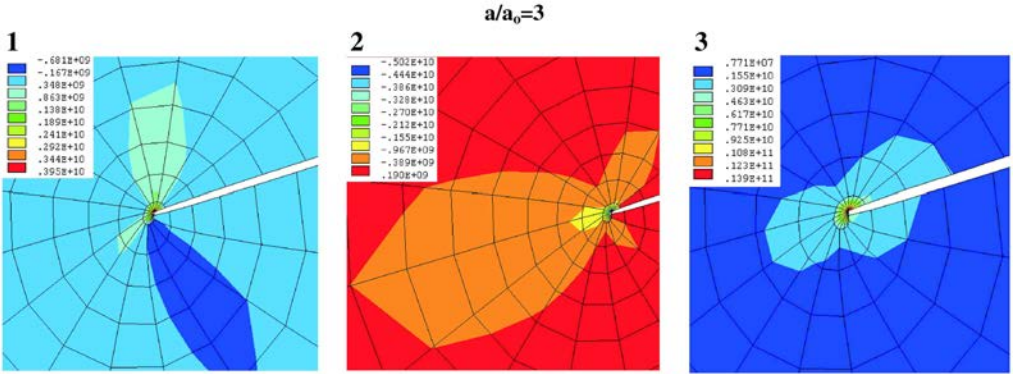


FIG. 12. Near-crack tip stress distribution ($+\Delta E_2 = 10\%$) [Pa]
 (1) normal (2) shear (3) von Mises.

Then, it has been already mentioned that the lower layer thickness, h_2 , is the next, after E_2 , most important composite parameter that affects the composite fatigue life. However, it is not yet fully clear if the high value of the relative sensitivity is actually because of a large significance of that composite parameter, or it is rather caused by an increase in a load area. The latter fact obviously implies larger forces acting on the composite, that increase considerably the crack tip displacement and near tip stresses, and thereby the crack driving force. This leads finally to a serious reduction of the composite fatigue life. This issue must be investigated further, to conclude about an actual importance of h_2 on the composite fatigue life. It can be carried out by replacing the force (stress)-controlled loading conditions by displacement (strain)-controlled ones, hence avoiding any change in load when perturbing h_2 . Finally, the least important composite parameters are the interface radius and the Poisson's ratio of the lower component, R_I and ν_1 , respectively. The lack of significance of ν_1 and especially R_I is caused by the specific boundary conditions considered in this work. In a more general (complex) case of boundary conditions such as bending or compression, one might expect a much larger significance of composite curvature. Hence, the next step in application of the sensitivity analysis to composite fatigue delamination problems should consider other, more general boundary conditions.

It is believed that the information shown in Table 2 (particularly in the last line) might help a composite engineer to choose appropriate design directions to optimise the fatigue fracture performance of the composite. However, at the time being one should be careful with a direct translation of these results into design. It is due to the fact that the composite models used here, do not include other important composite parameters such as those connected with all inelastic damage micro-phenomena. Nevertheless, a change (enrichment) of the model

will not change the sensitivity approach presented in this work. It will solely introduce new design parameters in calculations. Hence, the results should be more useful with respect to composite design and optimisation.

4.4. Numerical stability of sensitivity analysis results

An important issue of sensitivity computations with the finite difference approach is the numerical stability of calculated sensitivities. Therefore, this aspect is briefly discussed herein. In order to analyse it, the sensitivities are calculated with respect to three different composite parameter increments, as it has been already mentioned above, i.e. promiles (0.001), percents (0.01) and tenths (0.1). Most of the sensitivities showed a very good numerical stability, i.e. the sensitivities computed for different parameter increments were nearly the same and did not show any oscillations (cf. Figs. 6–8). However, there were some cases in which the sensitivities were affected by parameter increments, as it is shown e.g. in Fig. 13 for the Young's modulus of the lower layer, E_2 . In that case, the sensitivities obtained for the largest parameter increment (+10%) were different from those calculated for smaller increments (+0.1 and 1.0%). Thus, the design parameter change equal to +10% was too large in the problem at hand to obtain reliable sensitivities. Therefore, the sensitivities were calculated once more for three increments using the central finite differences. The outcome is shown in Fig. 14, where the parameter-increment dependence is absent as compared with Fig. 13. Thus, on the one hand it shows that the dependences are caused by too large parameter increments, which is a common feature associated with an application of the forward finite difference approach. On the other hand, it points out that if any numerical instabilities arise due to the utilisation of that approach, then a user might avoid it by switching it to the central finite differences.

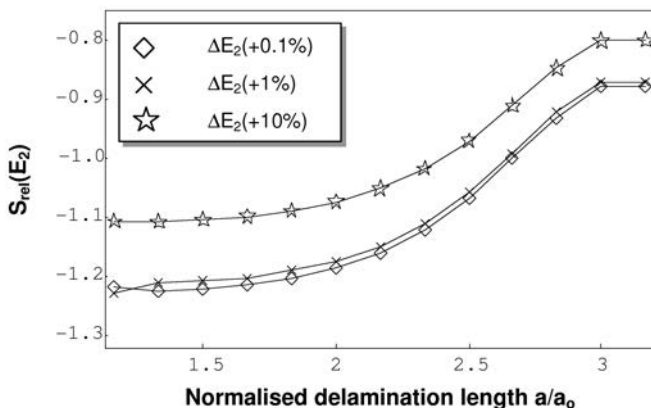


FIG. 13. Relative sensitivities of the fracture parameter with respect to the Young's modulus E_2 – forward finite difference.

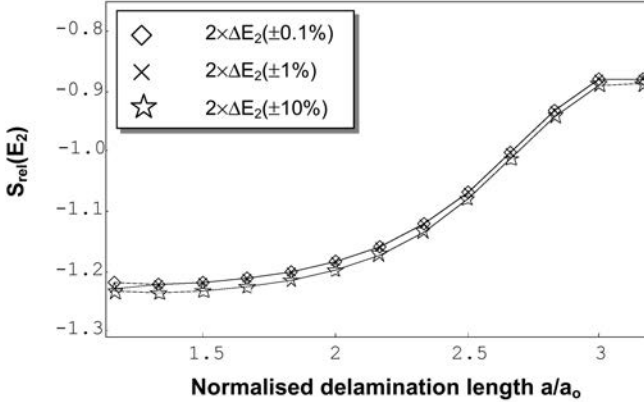


FIG. 14. Relative sensitivities of the fracture parameter with respect to the Young's modulus E_2 – central finite difference.

In general it was observed that the relative sensitivities of G_T and N_i obtained from the forward difference approach showed a good numerical stability for the parameter increment ($+1\%$).

4.5. Verification of relative sensitivities

Another important aspect was to verify the accuracy of calculated relative sensitivities with other existing approaches. Since no closed-form solution related to the problem considered was found, the numerical probabilistic approach reported in [24] was taken as a reference case. The reference approach is based on the Monte–Carlo simulation concept that helps to generate a design parameter spectrum according to a specified statistical distribution. Then, FEM-based simulations are run for each generated parameter from which the corresponding fracture parameters are calculated. Then, functions describing relations between the design and objective parameters (such as crack driving force) are numerically evaluated, differentiated with respect to a design parameter and normalised to obtain relative sensitivities.

Herein, the relative sensitivity values of the total energy release rate with respect to the Young's modulus of the lower layer, E_2 , are compared. Results from both approaches are collected in Table 3 as a function of the normalised delamination length. The sensitivities from the current (finite-difference) approach were calculated for the parameter increment $+1\%$.

It is shown in Table 3 that results from both approaches are in a very good agreement – sensitivities obtained from the reference approach are only slightly higher, especially for larger delamination lengths. This confirms the conclusion that current sensitivity calculations are correct from the computational point of view.

Table 3. Relative sensitivities of the total energy release rate G_T .

a/a_o	$S_{\text{rel}}(E_2)$	
	Current approach	Reference approach
1.0	-1.210	-1.230
1.167	-1.228	-1.226
1.333	-1.211	-1.225
1.5	-1.207	-1.220
1.667	-1.200	-1.214
1.833	-1.190	-1.203
2.0	-1.173	-1.186
2.167	-1.148	-1.160
2.333	-1.110	-1.122
2.5	-1.058	-1.069
2.667	-0.992	-1.003
2.833	-0.923	-0.933
3.0	-0.923	-0.933
3.167	-0.872	-0.933
3.333	-0.872	-0.933

5. CONCLUSIONS

A computational approach to sensitivity analysis was proposed in this work to study composite parameter effects in a fatigue delamination problem of a two-layer composite. The main conclusions that stem from this work are as follows:

1. The calculated relative sensitivities enabled to point out, both qualitatively as well as quantitatively, the importance (or lack of importance) of composite parameters, such as layer Young's modulus or thickness, on the fatigue life of a delaminated composite subjected to shear fatigue loads of constant amplitude. Results of the current investigation revealed an important fact that the relative sensitivities of the fracture parameter and fatigue cycle number are not constant but vary during delamination growth.
2. Relative sensitivities determined by the forward finite difference concept showed a satisfactory numerical stability – i.e. results were generally independent of the composite parameter increment. In cases where relative sensitivity results were parameter increment-dependent, the application of the central finite difference concept improved considerably their numerical

stability. However, in nearly all cases it was possible to find the appropriate parameter increment when using the forward finite differences.

3. Relative sensitivity values obtained from the current approach were verified and found to be in a very good agreement with relative sensitivity results of a sample-based approach to sensitivity analysis.
4. ANSYS post-processing environment appeared as a very convenient tool in implementing and executing the sensitivity analysis by solely using its parametric design language without a direct access to its source code. More computational details and parts of the implementation can be found in [20].
5. Actually it is not possible to conclude that the current approach can be applied to carry out the sensitivity analysis of other delamination problems in composite laminates. Therefore, it would be interesting and necessary to consider other, more general, boundary conditions such as cyclic bending or compression. This issue is left for future research.

REFERENCES

1. B. HARRIS [Ed.], *Fatigue in Composites*, CRC Press/Woodhead Publishing, 2003.
2. A. C. GARG, *Delamination – a damage mode in composite structures*, Eng. Fract. Mech., **29**, 557–584, 1988.
3. V. V. BOLOTIN, *Mechanics of Fatigue*, CRC Press, 1999.
4. Ł. FIGIEL, M. KAMIŃSKI, *Mechanical and thermal fatigue delamination in curved layered composites*, Comput. Struct., **81**, 1865–1873, 2003.
5. Ł. FIGIEL, N. E. ZAFEIROPOULOS, B. LAUKE, *Numerical analysis of the elastic constants' effects on the delamination propagation in a curved layered composite beam under cyclic shear loading*, Compos. Part A Appl-S, **A36**, 153–162, 2005.
6. H. J. HAUG, K. K. CHOI, V. KOMKOV, *Design Sensitivity Analysis of Structural Systems*, Academic Press, 1986.
7. S. KIBSGAARD, *Sensitivity analysis – the basis for optimisation*, Int. J. Numer. Meth. Eng., **34**, 901–932, 1992.
8. M. KLEIBER, H. ANTUNEZ, T. D. HIEN, P. KOWALCZYK, *Parameter Sensitivity in Non-linear Mechanics: Theory and Finite Element Computations*, John Wiley & Sons, 1997.
9. M. KAMIŃSKI, *Computational mechanics of composite materials. Sensitivity, randomness and multiscale behaviour*, Springer Verlag, 2005.
10. J. FISH, A. GHOULLI, *Multiscale analytical sensitivity analysis for composite materials*, Int. J. Numer. Meth. Eng., **50**, 1501–1520, 2001.
11. Ł. FIGIEL, M. KAMIŃSKI, *Fatigue sensitivity analysis for the curved composite beam*, pp. 477–484, [in:] *Brittle Matrix Composites 7*, A. M. BRANDT, V. LI, I. C. MARSHALL [Eds.], Woodhead Publishing, 2003.
12. M. E. M. EL-SAYED, E. H. LUND, *Structural optimization with fatigue life constraints*, Eng. Fract. Mech., **37**, 1149–1156, 1990.

13. M. KAMIŃSKI, *On probabilistic fatigue models for composite materials*, Int. J. Fatigue, **24**, 477–495, 2002.
14. J. S. ARORA, *Introduction to Optimum Design*, 2-nd Edition, Academic Press, 2004.
15. E. LAPORTE, P. LE TALLEC, *Numerical Methods in Sensitivity Analysis and Shape Optimisation*, Birkhäuser, Boston 2003.
16. A. GRIEWANK, *Evaluating Derivatives: Principles and Techniques of Algorithmic Differentiation*, Frontiers in Applied Mathematics 19, SIAM, 2000.
17. E. LUND, *FEM-based Design Sensitivity and Optimisation*, PhD thesis, Aalborg University, Denmark, 1994.
18. T. BURCZYŃSKI, *Applications of BEM in sensitivity analysis and optimisation*, Comput. Mech., **13**, 29–44, 1993.
19. K. DEMS, Z. MRÓZ, *Sensitivity analysis methods* [in Polish], pp. 647–721, [in:] *Handbook of Computational Solid Mechanics*, M. KLEIBER [Ed.], PWN, 1995.
20. Ł. FIGIEL, *Sensitivity analysis of interface fatigue crack propagation in elastic composite laminates*, PhD Thesis, Technical University of Dresden, SLUB Dresden, 2004.
21. J. W. HUTCHINSON, Z. SUO, *Mixed Mode Cracking in Layered Materials*, Adv. Appl. Mech., **29**, 63–191, 1992.
22. W. QIAN, C. T. SUN, *A frictional interfacial crack under combined shear and compression*, Composites Sci Technol., **58**, 1753–1761, 1998.
23. P. M. FRANK, *Introduction to System Sensitivity Theory*, Academic Press, 1978.
24. Ł. FIGIEL, M. KAMIŃSKI, *Deterministic and probabilistic sensitivity analysis of fatigue fracture for a curved two-layer composite*, Lecture Series on Computer and Computational Sciences, **4**, 1062–1064, Brill Academic Publishers, Leiden 2005.
25. J. SCHÖN, *A model of fatigue delamination in composites*, Composites Science and Technology, **60**, 553–558, 2000.
26. Ł. FIGIEL, M. KAMIŃSKI, B. LAUKE, *Analysis of a compressive shear fracture test for curved interfaces in layered composites*, Eng. Fract. Mech., **71**, 967–980, 2004.
27. I. S. RAJU, *Calculation of strain-energy release rates with higher order and singular finite elements*, Engineering Fracture Mechanics, **28**, 3, 251–274, 1987.

Received January 30, 2007; revised version October 26, 2007.
